Possibility of Flat-Band Ferromagnetism in Hole-Doped Pyrochlore Oxides $Sn_2Nb_2O_7$ and $Sn_2Ta_2O_7$

I. Hase, T. Yanagisawa, and Y. Aiura
National Institute of Advanced Industrial Science and Technology (AIST), Tsukuba Central 2, 1-1-1 Umezono, Tsukuba 305-8568, Japan

K. Kawashima
IMRA, Material R&D Co. Ltd., 2-1 Asahi-machi, Kariya, Aichi 448-0032, Japan

(Received 6 July 2017; published 7 May 2018)

Quantum mechanics tells us that the hopping integral between local orbitals makes the energy band dispersive. In a lattice with geometric frustration, however, dispersionless flat bands may appear due to quantum interference. Several models possessing flat bands have been proposed theoretically, and many attracting magnetic and electronic properties are predicted. However, despite many attempts to realize these models experimentally, compounds that are appropriately described by this model have not been found so far. Here we show that pyrochlore oxides $Sn_2Nb_2O_7$ and $Sn_2Ta_2O_7$ are such examples, by performing first-principles band calculation and several tight-binding analyses. Moreover, spin-polarized band calculation shows that the hole-doped systems $Sn_2Nb_2O_6N$ and $Sn_2Ta_2O_6N$ have complete spin polarization, and their magnetic moments are mostly carried by Sn-s and N-p orbitals, which are usually nonmagnetic. These compounds are not only candidates for ferromagnets without a magnetic element, but also will provide an experimental platform for a flat-band model which shows a wide range of physical properties.

DOI: 10.1103/PhysRevLett.120.196401

Geometric frustration causes various interesting properties. Let us consider a Hubbard model on a lattice, which is drawn as a line graph of a bipartite lattice [1]. Such a class of lattice includes a checkerboard lattice, kagome lattice, and pyrochlore lattice. The one-electron part of this Hubbard model has a flat band, which has no dispersion in the whole k space [2,3]. This anomalous flat band comes from quantum interference of the wave function, caused by the geometric frustration. This model (Mielke model or frustrated Hubbard model) has attracted much attention, and many interesting magnetic and electronic properties are theoretically proposed for this model, including rigorous ferromagnetism, curious topological invariant, quantum Hall effect, and superconductivity [1–6].

On the other hand, in the large on-site repulsion (U) limit, we can derive the frustrated Heisenberg model as an effective spin Hamiltonian [2]. Because of the strong magnetic frustration, this model shows various nontrivial magnetic properties [7]. In fact, it is experimentally known that some pyrochlore oxides exhibit curious magnetic properties, which include quantum spin liquid, spin ice, and magnetic monopole [8–12].

Stimulated by the theoretical predictions, and by the great success of the experimental findings of the frustrated Heisenberg model, experimental exploration of materials applicable to the Mielke model has also been carried out. For example, a kagome lattice has been artificially realized using a photonic crystal and a quantum wire [13–15]. There is also an attempt to realize a Hubbard model on a kagome lattice using a cold atom [16]. However, no bulk compound described by the Mielke model has been found, and no ferromagnetic ground state predicted by Mielke [1] has been reported yet.

In this Letter we investigated the electronic structure of pyrochlore oxides $Sn_2T_2O_7$ (T = Nb, Ta) for stoichiometric and hole-doped phases based on first-principles calculation. These compounds are given much attention as a candidate of photocatalytic materials and transparent conducting oxide [17–19]. Here we explain the crystal structure of pyrochlore oxides. The chemical composition is written by $A_2B_2O_7$, and is often written as $A_2B_2O_6O$ because there are two oxygen sites. $A_2B_2O_6O$ consists of a B_2O_6 unit formed by a corner-shared BO_6 octahedra and an A_2O unit formed by corner-shared A_4O tetrahedra. When we extract the A site, they form a geometric frustrated lattice (pyrochlore lattice). In the pyrochlore oxide $R_2Ti_2O_7$ (R is a rare-earth element), a magnetic and localized R^{3+} ion occupies the A site, and other ions form a closed shell and become inert. Thus, $R_2Ti_2O_7$ is an ideal system which realizes the Heisenberg model on a geometric frustrated lattice and shows a rich magnetic phase diagram as shown above.

We show that the valence band maximum (VBM) of $Sn_2T_2O_7$ has a characteristic quasi-flat band, and it can be well described by a tight-binding model which includes Sn-s and O′-p orbitals with nearest-neighbor hopping. This

tight-binding model has a flat-band as in the Mielke model. Combined with the result that the ferromagnetic ground state survives when the flat band is slightly distorted [20,21], we can expect that hole-doped $Sn_2T_2O_7$ may have a ferromagnetic ground state. In order to verify this idea, we also performed a first-principles calculation including spin degree of freedom for the hole-doped $Sn_2T_2O_7$. As expected, we obtained a ferromagnetic ground state for them. Interestingly, the spin polarization is carried by Sn and O atoms, which are usually nonmagnetic.

We have calculated the electronic structure of $Sn_2T_2O_7$ (T = Nb, Ta) from first principles for nondoped and hole-doped cases. Details of the calculations are described in Ref. [22].

Figure 1(a) shows the density of states (DOS) curve of $Sn_2Nb_2O_7$. As expected from the ionic configuration $Sn_2^{+2}Nb_2^{+5}O_7^{-2}$, it becomes an insulator. The magnitude of the band gap (0.925 eV) is about a half of the experimental value 2.3 eV [17], due to the underestimation of the band gap by density-functional calculation. The DOS curve of $Sn_2Ta_2O_7$ (not shown) is essentially similar to that of $Sn_2Nb_2O_7$, except for the larger band gap 1.33 eV. The experimental optical gap of $Sn_2Ta_2O_7$ is 3.0 eV. Our calculation results show good agreement with previous works [17,27]. The VBM shows a very characteristic sharp DOS feature just below the Fermi level (E_F). The bands with energy 0 to −3 eV are mainly composed of Sn-s and O-p orbitals. We show the band dispersion of $Sn_2Nb_2O_7$ near E_F in Fig. 1(b). From this band dispersion, it is seen that the sharp VBM feature shown in Fig. 1(a) is caused by

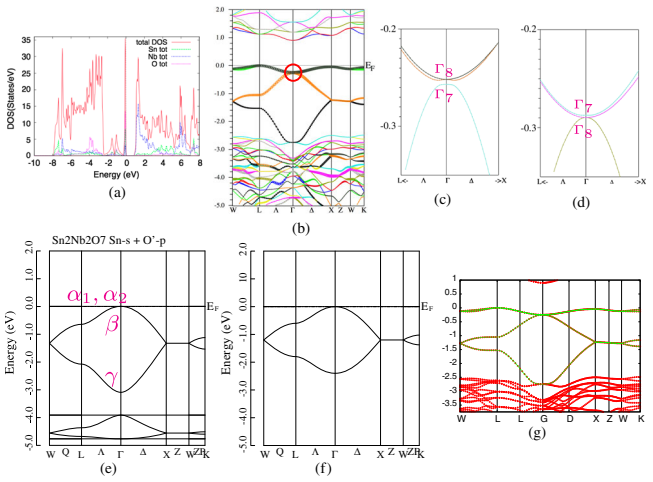

FIG. 1. (a) DOS curve and (b) energy dispersion of $Sn_2Nb_2O_7$ from the first principles. As for the partial DOS, we only show Sn, Nb, and O′ states for clarity. In (b), the thickness of the lines represents the amount of the O′-p component. (c),(d) A zoom-up view near Γ point shown by the circle in (b) for (c) $Sn_2Nb_2O_7$ and (d) $Sn_2Ta_2O_7$. (e),(f) Energy dispersion of the (e) 10-orbital and (f) 4-orbital tight-binding model. (g) MLWF fitting with 4 orbitals. The unit of energy is eV. E_F is set as 0 eV or the VBM. The parameters used in (e)–(g) are shown in Table I and Ref. [22].

nearly degenerated two bands with narrow band width from E_F to −0.3 eV, where the maximum splitting is ∼0.04 eV along the W-Q-L axis. Note that the band gap is an indirect one for these two compounds (VBM is at the L point, while the conduction band minimum is at the Γ point).

Since the flat-band system may cause interesting behavior by the spin-orbit interaction (SOI) [3], we also performed a band calculation with SOI [22]. Figure 1(c) shows a zoom-up near the Γ point shown by the circle in Fig. 1(b). Without SOI, the quasi-flat band touches the dispersive band at this Γ point [28]. In $Sn_2T_2O_7$, the state of this point is specified by the threefold (sixfold if we include spin) degenerated Γ_{25} irreducible representation without SOI. When SOI is included, this state splits into twofold Γ_7 and fourfold Γ_8 states as in Fig. 1(c) for $Sn_2Nb_2O_7$ and Fig. 1(d) for $Sn_2Ta_2O_7$. Interestingly, in the case of $Sn_2Ta_2O_7$, the order of Γ_7 and Γ_8 is reversed and there is no band gap even including SOI. This is in contrast to the case of a recently predicted 2D kagome lattice formed by a metal-organic framework (MOF) [29], which has a clear band gap at the Γ point when including SOI. Hence, we can expect that the topological property of the quasi-flat band in $Sn_2Ta_2O_7$ is different from that in $Sn_2Nb_2O_7$ and 2D MOF.

Next, in order to grasp the electronic structure intuitively, we fitted these bands with energy 0 to −3 eV by a tight-binding model including Sn-s and O-p orbitals with nearest-neighbor transfer integrals [22], as shown in Fig. 1(e). Since the primitive unit cell (PUC) contains two formula units [i.e., $2(Sn_2T_2O_7)$ in PUC], this model includes 4 Sn-s orbitals and 6 O′-p orbitals (10-orbital model). Although this model is quite simple, the band dispersion is well described except the energy splitting in the L point. The VBMs with energy 0 eV (α_1, α_2) are doubly degenerated and *completely* flat in this model, as in the Mielke model. Interestingly, there are other flat bands with energy ~ -4.0 and ~ -5.0 eV, which mainly consist of O′-p orbitals. However, since these flat bands are hidden by other bands (mainly O-p bands), they may be difficult to observe. And since O′-p orbital energy is not so different from O-p orbital energy, strong hybridization with the dispersive O-p bands easily destroys the flatness of the O′-p bands.

In contrast, since the orbital energy of Sn-s and O-p are well separated, we can integrate out the O-p contribution and construct a tight-binding model including only Sn-s orbitals (4-orbital model) for the bands with energy 0 to −3 eV. The obtained band dispersion is shown in Fig. 1(f). This model is so simple that it contains only one parameter $t = (ss\sigma)$, and is exactly the same as the model proposed by Mielke [1]. Nevertheless, such a good agreement with the *ab initio* bands is quite impressive. Interestingly, when we go to the 4-orbital model, the dispersion of the bands α_1, α_2 and β except for the energy offset can be well described by simply removing O′-p orbitals and keeping ϵ_s and $(ss\sigma)$ the same. That is, the structure of these bands is hardly dependent on $(sp\sigma)$. However, for the lowest band γ in

Fig. 1(f), agreement with *ab initio* calculation is worse because $(sp\sigma)$ greatly affects the bandwidth. As for $Sn_2Ta_2O_7$, about a 10% increase of $(ss\sigma)$ can fit the Sn-s bands well.

In order to obtain a more precise description of the bands near E_F, we constructed maximum localized Wannier functions (MLWFs) using "Sn-s" orbitals [22]. We can perfectly reproduce the original bands as shown in Fig. 1(g), and the five largest parameters are shown in Table I. We found that the transfer integral of the first nearest-neighbor (t_1) determines the overall shape of the band dispersion, including the flat band. The t_2–t_4 gives this flat band an energy dispersion with ~0.3 eV, which is seen in the *ab initio* band.

To our knowledge, these compounds are the first examples in which flat bands derived from the frustrated lattice have appeared near E_F. Even though there are many pyrochlore oxides, in most of them the A site is not relevant to the electronic state around E_F. Or in some compounds, because the states other than s orbitals are involved, the model with isotropic transfer integrals cannot be applied. One exception is $Tl_2Ru_2O_7$ [30], whose Tl-s orbital is located near the VBM and its dispersion is similar to the Sn-s quasi-flat band in $Sn_2T_2O_7$. However, in $Tl_2Ru_2O_7$, Ru-d bands are partially occupied and they mask the anomaly of the Tl-s quasi-flat band. In $Sn_2T_2O_7$ there is no such complication, and this is an ideal system to see the flat band by a geometric frustrated lattice.

Next we discuss the hole-doping case. For a perfect flat-band system, if this flat band is partially filled, then the DOS at E_F diverges. In this case, the system becomes unstable against small perturbations, such as lattice distortion and spin polarization. In fact, Fujimoto shows that charge order with lattice distortion causes a metal-insulator transition for the Hubbard model on a 3D-pyrochlore lattice when the (perfect) flat band is half filled [31]. However, in $Sn_2Nb_2O_7$, we did not observe such a lattice distortion by x-ray diffraction experiment, at least at room temperature [18]. This may be due to the finite bandwidth of the quasi-flat band and/or due to the small carrier density of the sample. Therefore, hereafter we do not consider the lattice distortion, and focus on the spin polarization in hole-doped $Sn_2Nb_2O_7$.

In a perfect flat-band system it is rigorously shown that when the flat band is half filled, it has one and only one ferromagnetic ground state with *any* value of U [1]. Even in the system with quasi-flat bands, a numerical study has shown that a ferromagnetic ground state is realized under sufficiently large U [20]. The criterion of U that divides the ferromagnetic and paramagnetic ground state is $U \sim W$, where W denotes the width of the quasi-flat band. It is not easy to estimate U on the Sn-s Wannier orbital quantitatively, but it is plausible to expect that U is larger than $W \sim 0.3$ eV in this case. For example, it is considered that even U on the oxygen cite (U_p) has 2–4 eV magnitude [32,33]. There is also an exact result that the ferromagnetic ground state is stable for a slight bending of the flat band [21].

Next, we show the *ab initio* calculation results for the hole-doped $Sn_2T_2O_7$. We tried hole doping in two ways. First, replace O with N. Second, replace Nb with a hypothetical atom Nz, which has a fractional number of electrons and nuclear charge [virtual crystal approximation (VCA)]. This VCA models the substitution of Nb^{5+} by Zr^{4+}, but the substitution of Nb^{5+} by excess Sn^{4+} may have similar hole-doping effect [18].

Figure 2 shows the band dispersion of $Sn_2Ta_2O_6N$. There is an exchange splitting of the up-spin and down-spin valence band. All the extra hole carriers occupy the down-spin band; i.e., this system is half-metallic. Therefore, the total magnetic moment becomes $M = 2.00\mu_B$. As described above, since the structure of this band hardly depends on $(sp\sigma)$, even if O′ is replaced by N, the band

TABLE I. Tight-binding parameters for several models for $Sn_2Nb_2O_7$. (a) 10-orbital and 4-orbital models including only nearest-neighbor hopping. As for the 4-orbital model, we simply omit O′-p orbitals from the 10-orbital model and adjust the offset by modifying ϵ_s. (b) 4-orbitals MLWF model. The detail of the notation is shown in Ref. [22]. All the units of energy are eV.

(a)		10-orbital	4-orbital
	ϵ_s	−1.4	−0.600
	ϵ_p	−3.9	⋯
	$(ss\sigma)$	−0.28	−0.28
	$(sp\sigma)$	1.12	⋯

(b)	$\mathbf{R}_i^\mu - \mathbf{R}_j^\nu$	(i,j)	ϵ, t	Deg	Distance
ϵ	(0,0,0)	(1,1)	−0.7037	×1	On site
t_1	(0,0,0)	(1,2)	−0.2764	×6	$0.3536a$
t_2	(−1, 1, 0)	(1,1)	−0.0366	×6	$0.7071a$
t_3	(1,0,0)	(1,1)	0.0153	×6	$0.7071a$
t_4	(−1, 0, 1)	(1,2)	0.0130	×6	$0.6123a$

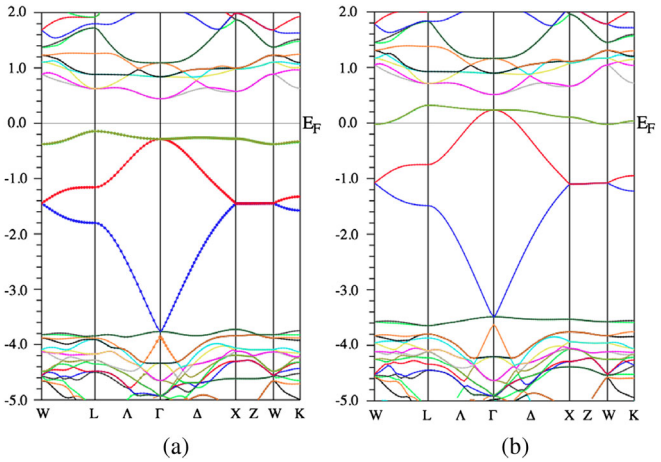

FIG. 2. Energy dispersion of $Sn_2Ta_2O_6N$ for (a) up spin and (b) down spin.

shape hardly changes. However, since the energy of the N-p orbital is shallower than that of the O′-p orbital, the band gap becomes smaller. As for $Sr_2Nb_2O_6N$, the band gap collapses for the down-spin band (not shown), but still has $M = 2.00\mu_B$.

Also in the case of VCA, the shape of the valence band hardly changes when δ (the number of holes per Nb) is smaller than 0.5. When we substitute Nb to Nz, the nuclear charge decreases and the energy level of the conduction band becomes shallower. However, for the valence band there is only little change from the original one. As a result, the band gap increases.

The dependence of M on δ in hole-doped $Sn_2Nb_2O_7$ is shown in Fig. 3. The number of holes is controlled by VCA. First, we focus on the case where u is fixed at 0.4349, which is the optimized value for the pristine $Sn_2Nb_2O_7$ (filled squares). Although M initially increases in proportion to δ, it decreases conversely when δ exceeds 0.5 and becomes zero with $\delta = 1$. The point $\delta = 0.5$ is just where the quasi-flat band is half filled. This behavior looks like the Slater-Pauling curve [34,35], which is universally seen in various ferromagnetic alloys. The hole-poor side of the Slater-Pauling curve can be explained by a simple rigid band model. That is, since holes are present only in the down-spin band in this region, increasing electrons fill the holes and decrease M. Since the PUC of $Sn_2Nb_2O_7$ contains four Nb atoms, the "Slater-Pauling line" becomes $M = 4\delta$. We see that our calculated $M(\delta)$ well agrees with $M = 4\delta$. We also plotted M for $Sn_2Nb_2O_6N$ (T = Nb, Ta) by a filled circle, and obtained the full moment $M = 2.00\mu_B$ as shown above.

If the valence band merely consists of the quasi-flat band, the M versus δ plot will be symmetric for the line $\delta = 0.5$. We show the line $M = 4(1-\delta)$ in Fig. 3. However, the obtained $M(\delta)$ is asymmetric for the line $\delta = 0.5$. We may ascribe this asymmetry to the following reasons. First, there are dispersive bands below the quasi-flat band, which breaks the electron-hole symmetry assumed above. Second, the valence band feels the change of the conduction band by VCA through hybridization. In particular, W increases when we increase δ. As for $Sn_2Nb_2O_7$ and $Sn_2Nb_2O_6N$ (B site is occupied by Nb), W is about 0.3 eV. However, W is about 0.5 eV for $Sn_2Nz_2O_7$ with $\delta = 0.5$. Finally, the dispersive band [with energy -2.3– -0.6 eV in Fig. 1(b)] is merged into the O-p bands when we increase δ. As for $\delta > 0.6$, the tight-binding picture shown in Figs. 1(e) and 1(f) may no longer be appropriate.

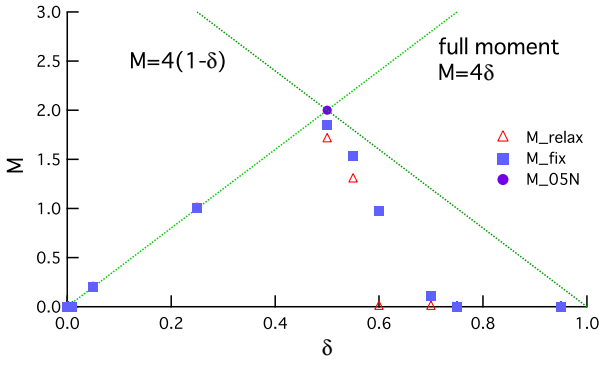

FIG. 3. Calculated magnetic moment M of hole-doped $Sn_2Nb_2O_7$ as a function of the doping level δ.

The magnitude of M also depends on the position of O atom u. The M versus δ plot obtained when u is optimized for each δ is also shown in Fig. 3 (open triangles). Although the Sn_2O network itself is not distorted, the shift of the O atom affects the effective transfer between Sn, then changes W, and eventually changes M. Therefore, when u is optimized for each δ, M decreases faster with increasing δ as compared with the fixed u case.

Our calculation is based on the Stoner model, which tends to overestimate the ferromagnetism. It is a future task to perform a more precise numerical many-body calculation using the model in Fig. 1(e) or 1(f) and appropriate Hubbard U. As for $\delta = 0.5$, we may also have to take care of the possible charge order [31]. Nevertheless, our results suggest that $Sn_2T_2O_7$ is a promising candidate for realizing the flat-band electronic state. We already have succeeded in synthesizing hole-doped $Sn_2(Nb, Ta)_2O_7$ samples [18,19]. However, the bands coming from the pyrochlore lattice, i.e., α, β, and γ bands in Fig. 1(e) are not observed in the photoemission spectra of these samples. Since other bands are clearly observed, we attribute this absence of the flat band to the deficiency of Sn atoms (∼10%) and O′ atoms (∼23%), which are considered to be very sensitive to the electronic structure near the VBM. Some numerical works suggest that the flat-band state is sensitive to disorder [36,37], though the calculation result for the 3D-pyrochlore lattice has not been reported yet.

Finally, we comment on the possibility that $Sn_2Nb_2O_7$ can behave like a magnetic 3D topological insulator. In the above discussion we show that the quasi-flat-band nature of $Sn_2Nb_2O_7$ is similar to 2D MOF [29]. In either case, the band gap opens by SOI and ferromagnetism is induced by some carrier doping. In this sense $Sn_2Nb_2O_7$ can be regarded as a 3D counterpart of the 2D MOF, in which quasi-flat band, ferromagnetism, and SOI naturally coexist. As for realizing the long-range magnetic order, a 3D material is apparently more suitable than a 2D material due to less fluctuation. In 2D MOF the quasi-flat band has the Chern number $c = 1$, which means that this band is topologically nontrivial [29]. It is also discussed that the fractional quantum Hall effect can occur in a 2D flat-band system [38–40]. The 3D counterpart material will pave the road to explore novel topological order. We further emphasize that $Sn_2Ta_2O_7$ belongs to a different class from $Sn_2Nb_2O_7$ because the former does not have a band gap when including SOI. The mixed compound $Sn_2(Ta, Nb)_2O_7$ has the possibility to show a topological phase transition, as seen in $(Bi, Sb)_2Te_3$ [41].

In summary, we found that the top of the valence band of $Sn_2T_2O_7$ (T = Nb, Ta) has quasi-flat-band nature. This anomalous band dispersion comes from the geometric frustration lattice of the Sn_2O network. Our first-principles calculation shows that various hole doping can induce ferromagnetism with nearly 100% spin polarization, and the magnetic moment mostly comes from Sn-s and O-p orbitals. These compounds are not only candidates for ferromagnets without magnetic elements, but also provide an experimental platform for flat band models showing a wide range of physical properties.

We thank H. Aoki, K. Kusakabe, H. Eisaki, F. Iga, A. Iyo, H. Kawanaka, K. Odagiri, and Y. Nishihara for fruitful discussions. This work was partially supported by KAKENHI (Grant No. JP26400379) from Japan Society for the Promotion of Science (JSPS).

[1] A. Mielke, J. Phys. A **24**, L73 (1991); **24**, 3311 (1991); **25**, 4335 (1992).
[2] O. Derzhko, J. Richter, and M. Maksymenko, Int. J. Mod. Phys. B **29**, 1530007 (2015).
[3] Z. Liu, F. Liu, and Y.-S. Wu, Chin. Phys. B **23**. 077308 (2014).
[4] Y. Hatsugai and I. Maruyama, Europhys. Lett. **95**, 20003 (2011).
[5] M. Kurita, Y. Yamaji, and M. Imada, J. Phys. Soc. Jpn. **80**, 044708 (2011).
[6] K. Kobayashi, M. Okumura, S. Yamada, M. Machida, and H. Aoki, Phys. Rev. B **94**, 214501 (2016).
[7] A. P. Ramirez, Annu. Rev. Mater. Sci. **24**, 453 (1994).
[8] B. Canals and C. Lacroix, Phys. Rev. Lett. **80**, 2933 (1998).
[9] A. P. Ramirez, A. Hayashi, R. J. Cava, R. Siddharthan, and B. S. Shastry, Nature (London) **399**, 333 (1999).
[10] C. Castelnovo, R. Mössner, and S. L. Sondhi, Nature (London) **451**, 42 (2008).
[11] H. Kadowaki, N. Doi, Y. Aoki, Y. Tabata, T. J. Sato, J. W. Lynn, K. Matsuhira, and Z. Hiroi, J. Phys. Soc. Jpn. **78**, 103706 (2009).
[12] K. Matsuhira, C. Paulsen, E. Lhotel, C. Sekine, Z. Hiroi, and S. Takagi, J. Phys. Soc. Jpn. **80**, 123711 (2011).
[13] F. Couny, F. Benabid, and P. S. Light, Opt. Lett. **31**, 3574 (2006).
[14] P. Mohan, F. Nakajima, M. Akabori, J. Motohisa, and T. Fukui, Appl. Phys. Lett. **83**, 689 (2003).
[15] K. Shiraishi, H. Tamura, and H. Takayanagi, Appl. Phys. Lett. **78**, 3702 (2001).
[16] J. Ruostekoski, Phys. Rev. Lett. **103**, 080406 (2009).
[17] Y. Hosogi, Y. Shimodaira, H. Kato, H. Kobayashi, and A. Kudo, Chem. Mater. **20**, 1299 (2008).
[18] Y. Aiura, K. Ozawa, I. Hase, K. Bando, H. Haga, H. Kawanaka, A. Samizo, N. Kikuchi, and K. Mase, J. Phys. Chem. C **121**, 9480 (2017).
[19] N. Kikuchi, A, Samizo, S. Ikeda, Y. Aiura, K. Mibu, and K. Nishio, Phys. Rev. Mater. **1**, 021601R (2017).
[20] K. Kusakabe and H. Aoki, Physica (Amsterdam) **194–196B**, 217 (1994).
[21] A. Tanaka and H. Ueda, Phys. Rev. Lett. **90**, 067204 (2003).
[22] See Supplemental Material at http://link.aps.org/supplemental/10.1103/PhysRevLett.120.196401 for details of the calculation, which includes Refs. [23–26].
[23] J. P. Perdew, K. Burke, and M. Ernzerhof, Phys. Rev. Lett. **77**, 3865 (1996).
[24] P. Blaha, K. Schwarz, G. K. H. Madsen, D. Kvashnicka, and J. Luitz, *WIEN2k, An Augmented Plane Wave + Local Orbitals Program for Calculating Crystal Properties* (Vienna University of Technology, Vienna, 2001).
[25] A. Yanase, *FORTRAN Program for Space Group TSPACE* (Shokabo, Tokyo, 1995) (in Japanese).
[26] A. A. Mostofi, J. R. Yates, Y.-S. Lee, I. Souza, D. Vanderbilt, and N. Marzari, Comput. Phys. Commun. **178**, 685 (2008).
[27] O. I. Velikokhatnyi and P. N. Kumta, ECS Trans. **28**, 37 (2010).
[28] D. L. Bergman, C. Wu, and L. Balents, Phys. Rev. B **78**, 125104 (2008).
[29] M. G. Yamada, T. Soejima, N. Tsuji, D. Hirai, M. Dincă, and H. Aoki, Phys. Rev. B **94**, 081102R (2016).
[30] F. Ishii and T. Oguchi, J. Phys. Soc. Jpn. **69**, 526 (2000).
[31] S. Fujimoto, Phys. Rev. B **67**, 235102 (2003).
[32] V. J. Emery, Phys. Rev. Lett. **58**, 2794 (1987).
[33] C. Weber, A. Läuchli, F. Mila, and T. Giamarchi, Phys. Rev. Lett. **102**, 017005 (2009).
[34] J. C. Slater, Phys. Rev. **49**, 537 (1936).
[35] L. Pauling, Phys. Rev. **54**, 899 (1938).
[36] J. T. Chalker, T. S. Pickles, and P. Shukla, Phys. Rev. B **82**, 104209 (2010).
[37] J. D. Bodyfelt, D. Leykam, C. Danieli, X. Yu, and S. Flach, Phys. Rev. Lett. **113**, 236403 (2014).
[38] T. Neupart, L. Santos, C. Chamon, and C. Murdy, Phys. Rev. Lett. **106**, 236403 (2011).
[39] D. N. Sheng, Z. C. Gu, K. Sun, and L. Sheng, Nat. Commun. **2**, 389 (2011).
[40] N. Regnault and B. A. Bernevig, Phys. Rev. X **1**, 021014 (2011).
[41] J. Zhang *et al.*, Nat. Commun. **2**, 574 (2011).